Impact of Conformational Transitions on SPR Signals-Theoretical Treatment and Application in Small Analytes/Aptamer Recognition

Jérôme Dejeu, Hugues Bonnet, Nicolas Spinelli, Eric Defrancq, Liliane Coche-Guerente, Angéline van Der Heyden, P. Labbe

Impact of Conformational Transition on SPR Signals - Theoretical Treatment and Application to Small Analytes/Aptamer Recognition

Jérome Dejeu, Hugues Bonnet, Nicolas Spinelli, Eric Defrancq, Liliane Coche-Guérente, Angéline Van der Heyden* and P. Labbé*

Univ. Grenoble Alpes, CNRS, DCM, 38000 Grenoble, France

AUTHOR INFORMATION

Corresponding Author

* jerome.dejeu@univ-grenoble-alpes.fr, angeline.van-der-heyden@univ-grenoble-alpes.fr

ABSTRACT

Surface plasmon resonance is a powerful technique for label-free and real-time characterization of molecular interactions at interfaces. However, the detection of small molecules still remains a challenge. Here, we report on the direct detection of a low molecular weight compound by its receptor presented as a monolayer. Moreover, the signal observed is more than twice the expected mass-weighted response. To establish the origin of the signal enhancement, we present herein a theoretical model that simulates the maximal SPR response by taking into account the aptamer conformational change. We demonstrated that the thickness layer variation is not the only parameter to be considered. We highlighted that the conformational transition of the aptamer also induces a deviation of the refractive index increment (RII) of the target /aptamer complex from the sum of the RII of individual entities. This non-additivity of the RII significantly contributes to the magnitude of the signal. We also propose the prediction of the maximal SPR response in function of the penetration depth, the ratio of the mass-weighted RII of the partners, the sensing layer thickness and the correction of the complex RII. This model provides new insights in parameters to be considered for analysis of SPR signals.

INTRODUCTION

Aptamers are short synthetic oligonucleotides, single-stranded DNA or RNA, which have unique three-dimensional structures to bind their targets with high affinity and specificity. Aptamers have been selected by SELEX method (Systematic Evolution of Ligands by EXponential enrichment) for a wide range of targets from ions to whole cells including small organic molecules and proteins.[1, 2] In comparison with antibodies, aptamers present advantageous

properties such as their easy chemical synthetic accessibility, their thermal and chemical stabilities. Therefore, aptamers have already found applications in various domains such as diagnostics,[3] therapy[4] or drug delivery[5, 6] and have emerged as very attractive candidates for the design and development of biosensors especially for low molecular weight (LMW) analytes.[7-9] Indeed, LMW molecules represent a class of compounds with high level of interest since it includes toxins, environmental pollutants or endocrine disruptors.[10]

Among the large choice of techniques for studying biomolecular interactions, SPR is a powerful tool enabling direct detection of binding events in real time and without labeling step.[11] Since SPR is based on the change of surface refractive index (RI), which is related to the molecular weight of the analyte, SPR detection of LMW molecules represents a challenge. The increase of the receptor density by its random 3D immobilization onto grafted hydrogels can overcome this limitation. In fact, this approach has been seldom employed for aptasensor[12, 13] while indirect strategies of detection are commonly reported. In these indirect assays, the main strategies are based on competitive [14, 15] or sandwich approaches involving either aptakiss[16, 17] or split aptamers where one subunit is grafted on the sensor and the complementary subunit is linked to metallic nanoparticles.[18, 19] However, it is well known, that due to the exponential decrease of the evanescent electric field intensity, the SPR detection is more sensitive for events occurring at a short distance from the gold layer surface. This property has been exploited in the present study that focuses on the feasibility of SPR direct detection of LMW analytes by a 2D aptamer platform. Our work describes as a proof of concept the recognition of *L*-tyrosinamide (*L*-Tym, MW 180.2 $g.mol^{-1}$) by a 49-mer oligonucleotide aptamer immobilized as an oriented monolayer. *L*-Tym was chosen as model since it is one of the lightest molecular weight molecules for which a highly selective aptamer has been selected. A significant SPR signal was observed allowing the

possibility to quantitatively evaluate the *L*-Tym/aptamer interaction. More interestingly, the SPR response was almost twice the predicted mass-weighted response.

To investigate the origin of the signal enhancement, we have developed a theoretical model that takes into account the aptamer folding upon recognition. Indeed, the conformation transition of the aptamer induces a reduction of the aptamer layer as already demonstrated.[20] SPR has been successfully used for monitoring conformational modification such as the thermal response of poly(*N*-isopropylacrylamide) brushes,[21] the denaturation and renaturation of self-assembled yeast iso-1-cytochrome.[22], the conformational dynamics of adsorbed poly(acrylic acid),[23] or proteins conformational changes such as for RNase A and Lysozyme.[24, 25] However, the use of receptor conformational changes for the detection of LMW molecules by SPR has scarcely been reported in the literature. An interesting study reported by Pitner *et al.* [26] indicated how the target-induced conformational change of a protein allows the detection of LMW molecules with the example of maltose binding protein (MBP) and tissue transglutaminase (tTG).[26] It was demonstrated that target binding can trigger a change in the hydrodynamic radius of the receptor, which in turn induces a SPR detectable change of the sensing layer refractive index. Negative responses have been observed in case of decrease of hydrodynamic radius of MBP upon interaction with maltose whereas positive responses have been observed in case of increase of the hydrodynamic radius of tTG upon interaction with calcium. In both cases, the variation of the signal induced by maltose or calcium exceeded the response expected for a mass-weighted response. In complement, the SPR detection of the calcium induced conformational change for four proteins has been in depth explored by Koch and coworker.[27-30] The authors demonstrated that the signal depends on the size variation of the protein as well as on variation of its hydration shells. With the theoretical model presented here, we proposed to evaluate the contribution of the various physical

parameters of the system on the final response. Our model highlights that the reduction of the sensing layer thickness is not sufficient to explain the experimental signal and that modification of the optical properties of the *L*-Tym/aptamer complex has to be also considered. To the best of our knowledge, this is the first example demonstrating that SPR transduction can be efficiently used to detect directly LMW compounds with aptamers immobilized as 2-D platform. Based on this example, a theoretical model is proposed to evaluate the contribution of conformational transition on the SPR response.

MATERIALS AND METHODS

Chemicals. Tris(hydroxymethyl)aminomethane (Tris), (11-Mercaptoundecyl)tetra(ethylene glycol) HS-$(CH_2)_{11}$-EG_4-OH, $MgCl_2$, NaCl, *L*-tyrosinamide and streptavidin, were purchased from Sigma-Aldrich. Polyoxyethylene sorbitan monolaurate (Tween 20®) was purchased from Euromedex, absolute ethanol was purchased from Acros, (11-Mercaptoundecyl)hexa(ethylene glycol) biotinamide HS-$(CH_2)_{11}$-EG_6-biotin was purchased from Prochimia (Poland). All aqueous solutions were prepared by using ultrapure water (Purelab UHQ) filtered (0.2 µm pore size). Experiment are performed in Tris buffer (20 mM Tris, 50 mM NaCl, 5 mM $MgCl_2$, 0.05% v/v Tween 20®, pH=7.5 in water). The oligonucleotides sequences were prepared as previously described.[20] Their sequences are the following: *L*-Tym aptamer, 5'AAT TCG CTA GCT GGA GCT TGG ATT GAT GTG GTG TGT GAG TGC GGT GCC C X3', X represents the 3' biotin TEG; random DNA sequence, 5'TGA TCA GAT GAG CGT TCC CAG CAC TTC AGC CGA CGA TGC AAC CAG TTT T X3', X represents the 3' biotin TEG (for ease of reading, this latter sequence is named "Scramble" in the text). Aliquots of oligonucleotides were dissolved in water

and stored at −20°C. Before each measurement, solutions of aptamer or random DNA sequence were prepared in Tris buffer, heated at 90°C and cooled overnight at room temperature.

Surface Plasmon Resonance. All SPR measurements were performed at 25°C in a Biacore T200 instrument (GE Healthcare). SPR bare gold sensor chips (SIA Kit AU) were from GE Healtcare. The gold sensor surface was rinsed with water, dried in a nitrogen gas stream and cleaned by 10 min UV-Ozone irradiation (Model 42-220; Jelight Conpany Inc.). The chip was then immersed for 15 min in high purity ethanol under stirring and dried in a nitrogen gas stream. The cleaned gold surface was then dipped overnight in a thiol solution (90% of 1mM HS-$(CH_2)_{11}$-EG_4-OH and 10% of 1mM HS-$(CH_2)_{11}$-EG_6-biotin) in ethanol. The surface was carefully cleaned with ethanol and dried with nitrogen. After thiol functionalization, the gold sensor chip was mounted inside the instrument and incubated in Tris buffer, used as running buffer (RB) in the whole experiment. The flow cells were modified by streptavidin injection (50 $\mu g.mL^{-1}$) at a flow rate of 30 $\mu L.min^{-1}$ during 15 min. Random DNA sequence and aptamer solutions were then injected respectively on the reference and active channels at a flow rate of 2 $\mu L.min^{-1}$ during 15 min until saturation near 600 RU. *L*-Tym solutions were successively injected for 2 min at a flow rate 30 $\mu L.min^{-1}$ at concentration of 10, 25, 50, 75, 100, 125, 150, 200, 300, 400, 500, 600, 700 and 1000 µM. Each *L*-Tym injection was followed by a 2 min running buffer rinsing step.

RESULTS

The *L*-Tym aptamer and a same size random DNA sequence monolayers (see sequences in the Materials and Methods part) were formed through streptavidin-biotin interactions. First, the gold surface was modified *ex-situ* by a mixed self-assembled monolayer (SAM) formed by co-adsorption of two pegylated (PEG) alkane thiols, one exhibiting a biotin terminal group. PEG were introduced to shield the surface towards non-specific adsorption while a 10% molar ratio of biotinylated thiol was selected to allow the formation of a saturated streptavidin (SA) layer.[31] Subsequently, the biotinylated aptamer and the random DNA sequence were anchored, respectively, on the sample and reference flow-cell until saturation. Finally, the recognition of *L*-Tym by the aptamer monolayer was evaluated by injection of *L*-Tym solutions at different concentrations on both flow-cells. Injection of *L*-Tym on the reference flow-cell led to square profiles (Figure S1A), the equilibrium response being linearly proportional to *L*-Tym concentration (see Figure SIB). Since *L*-Tym does not interact with the random DNA sequence,[20] this result suggests that *L*-Tym does not show nonspecific interaction with the underneath layer as well. Therefore, the signal measured on this reference flow-cell could be attributed exclusively to refractive index differences between the running buffer (RB) and injected *L*-Tym solutions that allows determination of the *L*-Tym RII ($\left(dn/dc\right)_A^{'}$ = 0.219 $cm^3.g^{-1}$). In contrast, curved profiles were recorded on the active flow-cell (Figure S2). Upon rinsing with RB, the signal returned to baseline meaning that the binding was completely reversible. The SPR signal responses related to the *L*-Tym specific interaction with the aptamer monolayer (figure 1A) were thus obtained after subtraction of the signals recorded on the reference flow-cell by applying a double referencing procedure.[32] It should be stressed that despite the LMW of *L*-Tym, its

interaction with the aptamer 2D platform led to an unexpected intense signal that allowed determination of the equilibrium dissociation constant of the interaction, Figure 1B. The adsorption isotherm was fitted in agreement with the 1:1 interaction mode of this recognition system.[33] The resulting equilibrium dissociation constant was K_D=103 ± 5 µM and the maximal response R_{max} was 17.9 ± 3.0 RU. In a satisfying way, similar values of R_{max} and K_D were obtained from kinetic data (see Figure S3 and Table S1). This K_D value is in the same order of magnitude as the one previously determined for a similar configuration by QCM-D.[20] It should be also noted that the K_D value obtained in our heterogeneous binding assays is higher than K_D values determined by other technics using homogeneous binding assays.[34,35,36] This difference could be explained by a surface crowding generated by the high concentration of the aptamer on the surface which hampers conformational transition that is necessary for the formation of the aptamer-target complex .

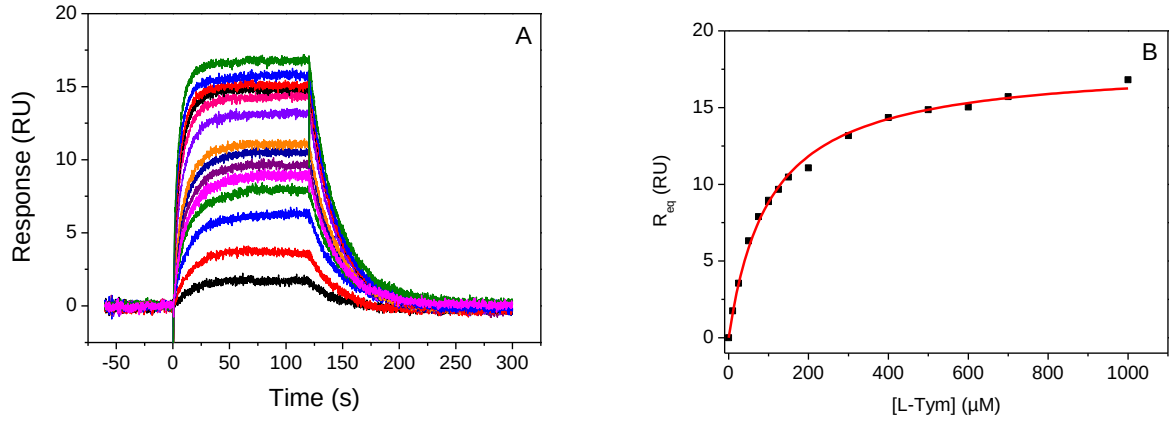

Figure 1. A) Double-reference subtracted sensorgrams recorded during the interaction of *L*-Tym (5 µM to 1 mM) with the aptamer monolayer in RB. T= 25°C. Flow rate: 30 µL/min. B) Adsorption isotherm (square) and fitting curve (line) using a 1:1 Langmuir interaction model.

Interestingly, the experimental maximal response recorded during the interaction (RU_{Amax}=17.9 RU) appears to be higher than the one expected considering the low molecular

weight of the target and the 2D presentation of the receptor. Indeed, the predicted response is only 7.9 RU according to Wilson formula (eq 1).[37]

$$R_{A_{max}} = RU_L \frac{MW_A.(dn/dc)'_A}{MW_L.(dn/dc)'_L} \times V = \beta.RU_L \times V \quad (1)$$

Where R_{Amax} is the predicted maximum response, RU_L is the amount of aptamer immobilized (560 RU), MW_A and MW_L are respectively the molecular weight of the analyte (*L*-Tym, 180.2 g.mol^{-1}) and of the immobilized ligand (aptamer, 15 831 g.mol^{-1}), $(dn/dc)'_A$ and $(dn/dc)'_L$ are the mass refractive index increments (RII) for *L*-Tym (0.219 cm^3.g^{-1} as calculated above) and for the aptamer (0.176 cm^3.g^{-1}) [38-41] respectively. $\beta = MW_A.(dn/dc)'_A / MW_L.(dn/dc)'_L$ is the ratio of the mass-weighted RII of the analyte *versus* the ligand (*i.e.* the ratio of the molar RII, see eqs S1 to S4) and *V*, the *Valency i.e.* the ratio number of analytes *per* number of ligands involved in the recognition (*V*=1 in the present system). Upon recognition, the aptamer undergoes a high structural rearrangement that triggers the decrease of the aptamer layer thickness from 5.2 nm to 3.8 nm as characterized by spectroscopic ellipsometry.[20] The intensity of the SPR signal being function of the distance from the surface, this reduction of almost 27% of the sensing layer has certainly an impact on the response and is not taken into account by the Wilson formula. To enlarge the latter formula, we proposed a new relationship (eq 18) that quantifies the contribution of aptamer conformational transition on SPR signal. To this end, we started from the initial equations of the SPR signal.[42, 43]

DISCUSSION

General expression of the SPR signal. In Biacore T200 SPR technology, a lens is used to focus the incident p-polarized light beam onto the prism base. Within the focus, a variety of angles of incidence are covered, ranging a few degrees around the resonance angle ϕ. Due to the presence of exponentially decreasing evanescent electric field intensity, SPR is sensitive to the effective refractive index of the medium in contact with the gold layer:[42, 43]

$$n_{eff} = \frac{1}{d_p} \int_0^{\infty} n(z) \exp\left(-z/d_p\right) dz \qquad (2)$$

Where ***n(z)*** is the refractive index at a distance z perpendicular to the sensor surface and $\boldsymbol{d_p}$ is the effective penetration depth of the SPR wave.

Figure 2 depicts schematically the two surfaces corresponding to the reference and the sample channel used in the present experiment.

A

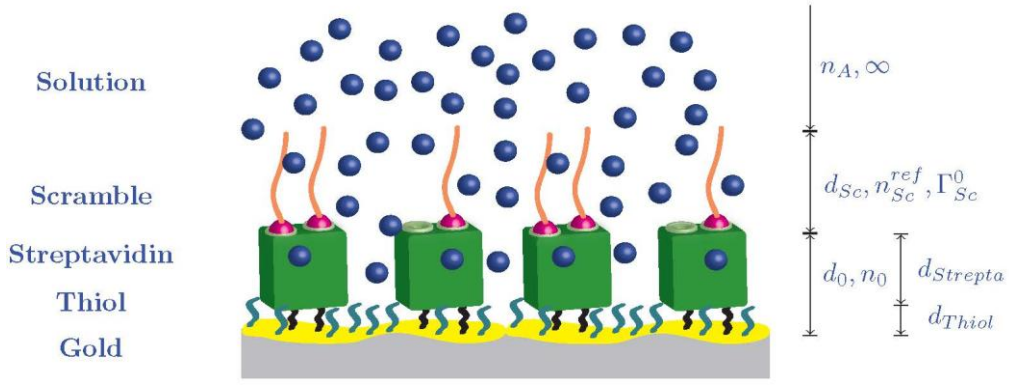

B

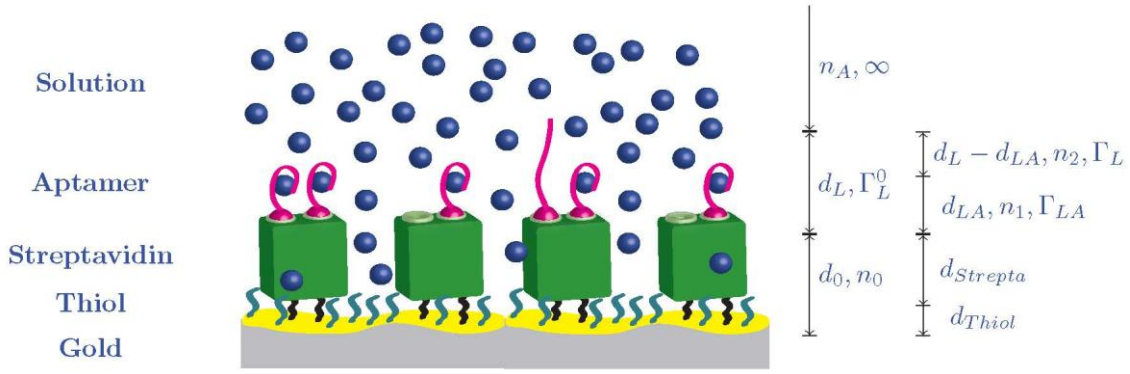

Figure 2. Schematic representation of: A) the reference flow-cell and B) the sample flow-cell. For clarity of the scheme, the free (non complexed) unfolded aptamer is presented in an elongated conformation, which should not correspond to the reality. $\boldsymbol{d_0}$ and $\boldsymbol{n_0}$ are respectively the thickness and the refractive index of the layer composed of the thiolated SAM and the SA. $d_L, \boldsymbol{\Gamma}_L^0$, are respectively the thickness and the surface density of the aptamer layer. $d_{Sc}, \boldsymbol{n}_{Sc}^{ref}$, $\boldsymbol{\Gamma}_{Sc}^0$ are respectively the thickness, the refractive index and the surface density of the layer formed by the random DNA sequence. $\boldsymbol{d_{LA}}$ and $\boldsymbol{n_1}$ are respectively the thickness and the refractive index of the folded aptamer under interaction with *L*-Tym. ($\boldsymbol{d_L}$ - $\boldsymbol{d_{LA}}$) and $\boldsymbol{n_2}$ are respectively the thickness and the refractive index of the layer formed by the unfolded aptamer. $\boldsymbol{n_i}$ is the refractive index of the injected solution.

Upon injection of *L*-Tym, the thickness of the aptamer layer decreases (figure 2B) whereas the one of the random DNA sequence remains unchanged (Figure 2A).[20] In details, according to *L*-Tym concentration and K_D, only a part of the aptamer is folded (eqs S12 to S14). The physical parameters of the different layer are listed in Table 1.

Table 1. Physical parameters involved in the recognition system.

	Refractive index (RI)	Thickness	Surface density	Refractive index increment (RII)
Scramble		d_{Sc}	Γ_{Sc}^{0}	$(dn/dc)_{sc}$
Aptamer before interaction		d_L	Γ_{L}^{0}	$(dn/dc)_{L}$
Free aptamer during interaction		d_L	Γ_{L}	$(dn/dc)_{L}$
L-Tym/aptamer complex		d_{LA}	Γ_{LA}	$(dn/dc)_{LA}$
Sublayer (SAM and SA)	n_0	d_0		
Scramble layer	n_{Sc}^{ref}	d_{Sc}		
Layer 1	n_1	d_{LA}		
Layer 2	n_2	d_L - d_{LA}		

The SPR response, R_A, attributed to the interaction of *L*-Tym with the aptamer layer is then defined as the difference (eq S9) between the effective refractive index of the active flow-cell (n_{eff}^{sample}, eq S7) and the one of the reference flow-cell (n_{eff}^{ref}, eq S8). After integration, the response is given by eq 3:

$$R_A = n_{eff}^{sample} - n_{eff}^{ref} = e^{-\frac{d_0}{d_p}}\left(n_1 - n_{Sc}^{ref}\right) + e^{-\frac{d_0+d_{LA}}{d_p}}\left(n_2 - n_1\right) + e^{-\frac{d_0+d_L}{d_p}}\left(n_i - n_2\right) + e^{-\frac{d_0+d_{Sc}}{d_p}}\left(n_{Sc}^{ref} - n_i\right) \qquad (3)$$

The refractive indexes can be replaced by their expression using De Feijter's relationship[44] (eq S11) that takes into account the composition of each layer. The reference cell is composed of the random DNA sequence so the refractive index of the aptamer layer is:

$$n_{sc}^{ref} = n_i + \left(\frac{dn}{dc}\right)_{Sc} \frac{\Gamma_{Sc}^0}{d_{Sc}} \tag{4}$$

The sample cell is composed of free aptamer (L) and of aptamer/*L*-Tym complex (LA). On the sample flow-cell, the refractive indexes of sublayers 1 and 2 are given by eqs 5 and 6 respectively:

$$n_1 = n_i + \left[\left(\frac{dn}{dc}\right)_{LA}\right] \frac{\Gamma_{LA}}{d_{LA}} + \left(\frac{dn}{dc}\right)_L \frac{\Gamma_L}{d_L} \tag{5}$$

$$n_2 = n_i + \left(\frac{dn}{dc}\right)_L \frac{\Gamma_L}{d_L} \tag{6}$$

Γ_{LA} and $\boldsymbol{\Gamma}_L$ are linked by $\boldsymbol{\theta}$, the ratio of aptamer entities in interaction with *L*-Tym *i.e.* the ratio of aptamer/*L*-Tym complexes amount versus $\boldsymbol{\Gamma}_L^0$ the total areal density of aptamer immobilized (eqs S12 to S14). Introducing θ and $\boldsymbol{\Gamma}_L^0$ in eqs 5 and 6, we obtained eqs 7 and 8.

$$n_1 = n_i + \left[\left(\frac{dn}{dc}\right)_{LA}\right] \frac{\theta\ \Gamma_L^0}{d_{LA}} + \left(\frac{dn}{dc}\right)_L \frac{(1-\theta)\ \Gamma_L^0}{d_L} \tag{7}$$

$$n_2 = n_i + \left(\frac{dn}{dc}\right)_L \frac{(1-\theta)\ \Gamma_L^0}{d_L} \tag{8}$$

After replacement of the different refractive index (eqs 4, 7 and 8) in eq 3, the response R_A can be separated in two terms (eq 9), R_{struct} (eq 10) and R_{int} (eq 11).

$$R_A = R_{struc} + R_{\text{int}} \tag{9}$$

$$R_{struc} = \left[e^{-\frac{d_0}{d_p}} \left(\left(\frac{dn}{dc}\right)_L \frac{\Gamma_L^0}{d_L} - \left(\frac{dn}{dc}\right)_{Sc} \frac{\Gamma_{Sc}^0}{d_{Sc}} \right) - e^{-\frac{d_0+d_L}{d_p}} \left(\frac{dn}{dc}\right)_L \frac{\Gamma_L^0}{d_L} + e^{-\frac{d_0+d_{Sc}}{d_p}} \left(\left(\frac{dn}{dc}\right)_{sc} \frac{\Gamma_{Sc}^0}{d_{Sc}} \right) \right] \tag{10}$$

$$R_{\text{int}} = \theta \left[e^{-\frac{d_0}{d_p}} \left(\left(\frac{dn}{dc}\right)_{LA} \frac{\Gamma_L^0}{d_{LA}} - \left(\frac{dn}{dc}\right)_L \frac{\Gamma_L^0}{d_L} \right) - \left(\frac{dn}{dc}\right)_{LA} \frac{\Gamma_A^0}{d_{LA}} e^{-\frac{d_0+d_{LA}}{d_p}} + \left(\frac{dn}{dc}\right)_L \frac{\Gamma_L^0}{d_L} e^{-\frac{d_0+d_L}{d_p}} \right] \tag{11}$$

The first term, R_{struc}, is independent of θ and refers only to the structure of both flow-cells before interaction. The second term, R_{int}, is function of θ and $\left(\boldsymbol{dn}/\boldsymbol{dc}\right)_{LA}$, and refers to the aptamer/*L*-Tym interaction. Thanks to a careful adjustment of the reference flow-cell with the random DNA sequence, application of a double referencing procedure cancelled the term $\boldsymbol{R_{struc}}$[32] and the residual SPR response corresponds to the interaction of *L*-Tym with the aptamer ($\boldsymbol{R_{int}}$) (eq 11).

Expression of the maximal SPR response. The maximal response R_{Amax} is obtained when all the aptamers on the surface are in interaction with *L*-Tym *i.e.* for θ = 1 (eq 12).

$$R_{A_{\max}} = e^{-\frac{d_0}{d_p}}\left(\left(\frac{dn}{dc}\right)_{LA}\frac{\Gamma_L^0}{d_{LA}} - \left(\frac{dn}{dc}\right)_{L}\frac{\Gamma_L^0}{d_L}\right) - \left(\frac{dn}{dc}\right)_{LA}\frac{\Gamma_L^0}{d_{LA}}e^{-\frac{d_0+d_{LA}}{d_p}} + \left(\frac{dn}{dc}\right)_{L}\frac{\Gamma_L^0}{d_L}e^{-\frac{d_0+d_L}{d_p}} \qquad (12)$$

Considering the RII of the complex *L*-Tym/aptamer as the sum of the RII of the individual entities (eq S6), and by introducing the folding ratio of aptamer ($\rho = d_{LA}/d_L$) in eq 12, the influence of the variation of the sensing layer is evidenced (eq 13).

$$R_{A_{\max}} = \frac{\Gamma_L^0}{d_L}\left(\frac{dn}{dc}\right)_{L} e^{-\frac{d_0}{d_p}}\left[\left(\frac{1}{\rho}-1\right) - \frac{1}{\rho}e^{-\frac{\rho d_L}{d_p}} + e^{-\frac{d_L}{d_p}}\right] + \frac{1}{\rho}\frac{\Gamma_L^0}{d_L}\left(\frac{dn}{dc}\right)_{A} e^{-\frac{d_0}{d_p}}\left[1 - e^{-\frac{\rho d_L}{d_p}}\right].V \qquad (13)$$

The maximal response can be then estimated in function of the experimental SPR signal recorded during the aptamer immobilization (RU_L) since the areal molar density of the aptamer (Γ_L^0) is linked to (RU_L) through the Jung's equation (eq S15). The expected SPR signal in the

case of modification of layer thickness coupled to the target recognition is thus expressed in eq 14.

$$R_{A_{\max}} = RU_L \left(\frac{1}{\rho} \frac{1 - e^{-\frac{\rho d_L}{d_p}}}{1 - e^{-\frac{d_L}{d_p}}} (\beta.V + 1) - 1 \right) \quad (14)$$

Based on eq 14, the expected maximal response that takes into account the target binding as well as the thickness variation of the aptamer layer is equal to 10.4 RU (with RU_L= 560 RU, dp=175 nm,[43] d_L=5.2nm[20] and ρ=0.73[20]). While reduction of the sensing layer contributes to the amplification of the SPR response, the theoretical response is still below the experimental maximal response (17.9 RU). In consequence, we hypothesized that modification of the tridimensional structure of the aptamer also induces a RII deviation of the *L*-Tym/aptamer complex from the sum of the RII of individual entities. Indeed, conformational changes of an immobilized receptor have an impact on the SPR detection of LMW molecules as seldom described in the literature. [26-30] In the reported studies, change of the hydrodynamic radius of protein and of its hydration shell is defined as the origin of the amplification. In line with our hypothesis, an interesting study carried out by backscattering interferometry, recently reported by Bornhop *et al*,[45] highlights that in recognition systems undergoing significant conformation or hydration changes, the RII value of the recognition complex is not equal to the sum of the RII values of two initial partners. Since the thickness decrease of the aptamer layer is not enough to originate the signal enhancement, we also assume a factor of correction of the refractive index increment of the aptamer/*L*-Tym complex.

Maximal SPR response in the case of thickness modification and of RII deviation. Considering a deviation factor for the RII of the analyte/ligand complex, eq 14 is not valid

anymore and a correction term has to be included. In consequence, the RII of the *L*-Tym/aptamer complex is expressed as a function of the aptamer one by introducing a correction factor, *x* (eq 15).

$$\left(\frac{dn}{dc}\right)_{correction} = x\left(\frac{dn}{dc}\right)_{L} \tag{15}$$

Where $(\boldsymbol{dn/dc})_{correction}$ is the correction of the *L*-Tym/aptamer complex RII defined as a function of the RII of the aptamer. By adding this correction factor to the sum of the RII of the two entities separately considered (eq S6), we obtain eq 16.

$$\left(\frac{dn}{dc}\right)_{LA} = \left(\frac{dn}{dc}\right)_{L} + V.\left(\frac{dn}{dc}\right)_{A} + \left(\frac{dn}{dc}\right)_{correction} = (1+x)\left(\frac{dn}{dc}\right)_{L} + V.\left(\frac{dn}{dc}\right)_{A} \tag{16}$$

This new expression of the *L*-Tym/aptamer complex RII is then introduced in eq 12 to obtain a new expression of maximal SPR response (eq 17).

$$R_{A_{\max}} = \frac{\Gamma_L^0}{d_L}\left(\frac{dn}{dc}\right)_{L} e^{-\frac{d_0}{d_p}}\left[\left(\frac{(1+x)}{\rho}-1\right)-\frac{(1+x)}{\rho}e^{-\frac{\rho d_L}{d_p}}+e^{-\frac{d_L}{d_p}}\right]+\frac{1}{\rho}\frac{\Gamma_L^0}{d_L}\left(\frac{dn}{dc}\right)_{A} e^{-\frac{d_0}{d_p}}\left[1-e^{-\frac{\rho d_L}{d_p}}\right].V \tag{17}$$

Noteworthy, the first term in eq 17 is related to the response generated by the aptamer folding and RII correction whereas the second term relies on target recognition. Again, using the Jung equation (eq S15), a new expression of the theoretically SPR signal taking into account the target recognition, the thickness layer variation and the correction of the *L*-Tym aptamer RII is obtained:

$$R_{A_{\max}} = RU_L\left(\frac{1}{\rho}\frac{1-e^{-\frac{\rho d_L}{d_p}}}{1-e^{-\frac{d_L}{d_p}}}(\beta\times V+1+x)-1\right) \tag{18}$$

Based on eq 18 and taking into account the experimental maximal response ($R_{A_{\max}} = RU_{A_{\max}} = 17.9\ RU$), a variation in the RII of the aptamer equal to 1.48% is calculated meaning an RII increase from 0.176 $cm^3.g^{-1}$ to 0.179 $cm^3.g^{-1}$. This RII variation is also in agreement to the one estimated from SE experiment (4%).[20] It should be noted that in absence of thickness modification (ρ=1) and of RII modification (x=0), eq 18 leads to the initial eq 1. Equation 18 is thus applicable to a wide range of recognition system where different configuration could be considered. If the recognition layer doesn't undergo a thickness modification but requires a RII correction coupled to the target recognition, eq 18 becomes:

$$R_{A_{\max}} = RU_L\left(\beta \times V + x\right) \tag{19}$$

In a more general way, our approach could be extended to the prediction of the maximal SPR response for systems that undergo conformational transition with or without thickness modification and/or with or without RII deviation.

Prediction of SPR response to system undergoing conformation modification. Based on equ 18, the impact of the various parameters (d_p, ρ d_L, β and x) on the maximal SPR response upon interaction can be evaluated under the dimensionless ratio R_{Amax}/RU_L. For fixed value of ρ, the penetration depth $\mathbf{d_p}$ of the evanescent electric field has low influence on the maximal SPR response (Figure 3A) on the 100 to 250 nm range. In the present study, considering dp equals to 175 nm,[43] a $\mathbf{d_p}$ variation of 10 nm induces an insignificant (less than 1%) variation of R_{Amax}/RU_L ratio (Figure S4).

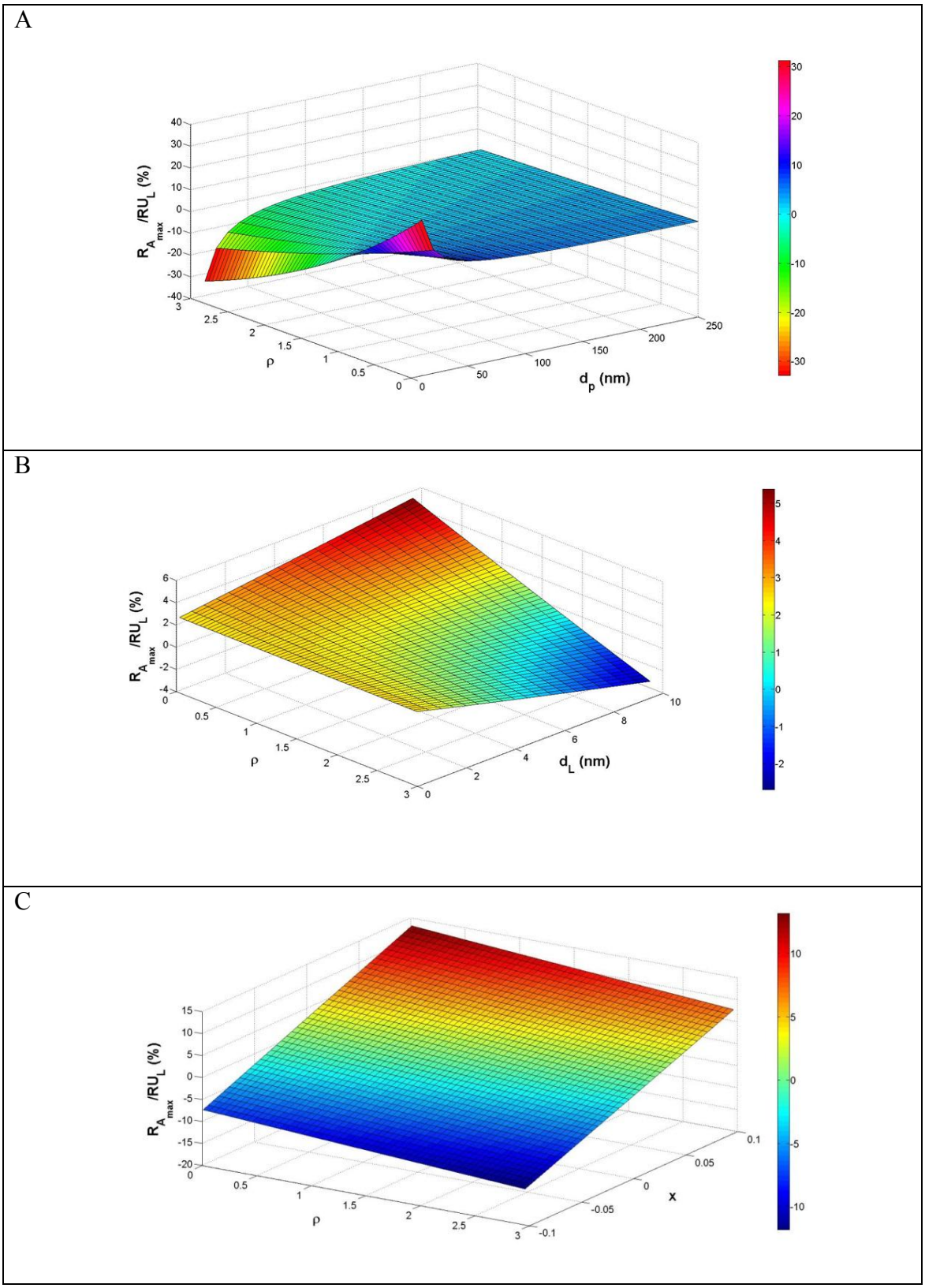

Figure 3. Variation of the R_{Amax}/RU_L ratio as a function of A) ρ and d_p B) ρ and dL C) ρ and x. The parameters are fixed to d_p=175nm, d_L=5.2 nm, ρ=0.73, β= 0.012 and x=0.01369.

Interestingly, the R_{Amax}/RU_L ratio linearly decreases with ρ whatever is the thickness of the initial recognition layer (Figure 3B). However, the slope of this dependence increases with the layer thickness. Variation of the layer thickness leads to either significant increase of the R_{Amax}/RU_L ratio in case of folding or significant decrease in case of elongation of the sensing layer. This observation is in concordance with previous work relating the SPR recognition of LMW analytes by protein undergoing large conformation change.[26] It should be noted that this negative ratio is also obtained in absence of layer thickness variations simply by considering a negative correction of the RII of the recognition complexes as exemplified by Figure 3C. The modulation of the signal by x is of crucial importance in our recognition system (β =0.012, d_L=5.7 nm), *e.g.* an increase of 2% of the RII of the complex leads to a 5 times enhancement. Figure 4 presents the influence of x in line with variation of the ratio of the mass-weighted RII, β. In the case of high value of β, *i.e.* the recognition of high molecular weight molecule by a LMW immobilized one, variations of x remain almost negligible on the R_{Amax}/RU_L ratio in comparison to the enhancement predicted for increasing values of β. However, correction of the RII appears to be a critical parameter in the case of recognition of LMW molecules by large receptors (β<0.5) as shown on Figure 4B (see also Figure S5 for β<1). A 10% increase of x extends the R_{Amax}/RU_L ratio by 20. This enhancement triggered by x correction of the complex RII allows analysis of LMW for those a low (or even non measurable) signal is predicted by eq 1.

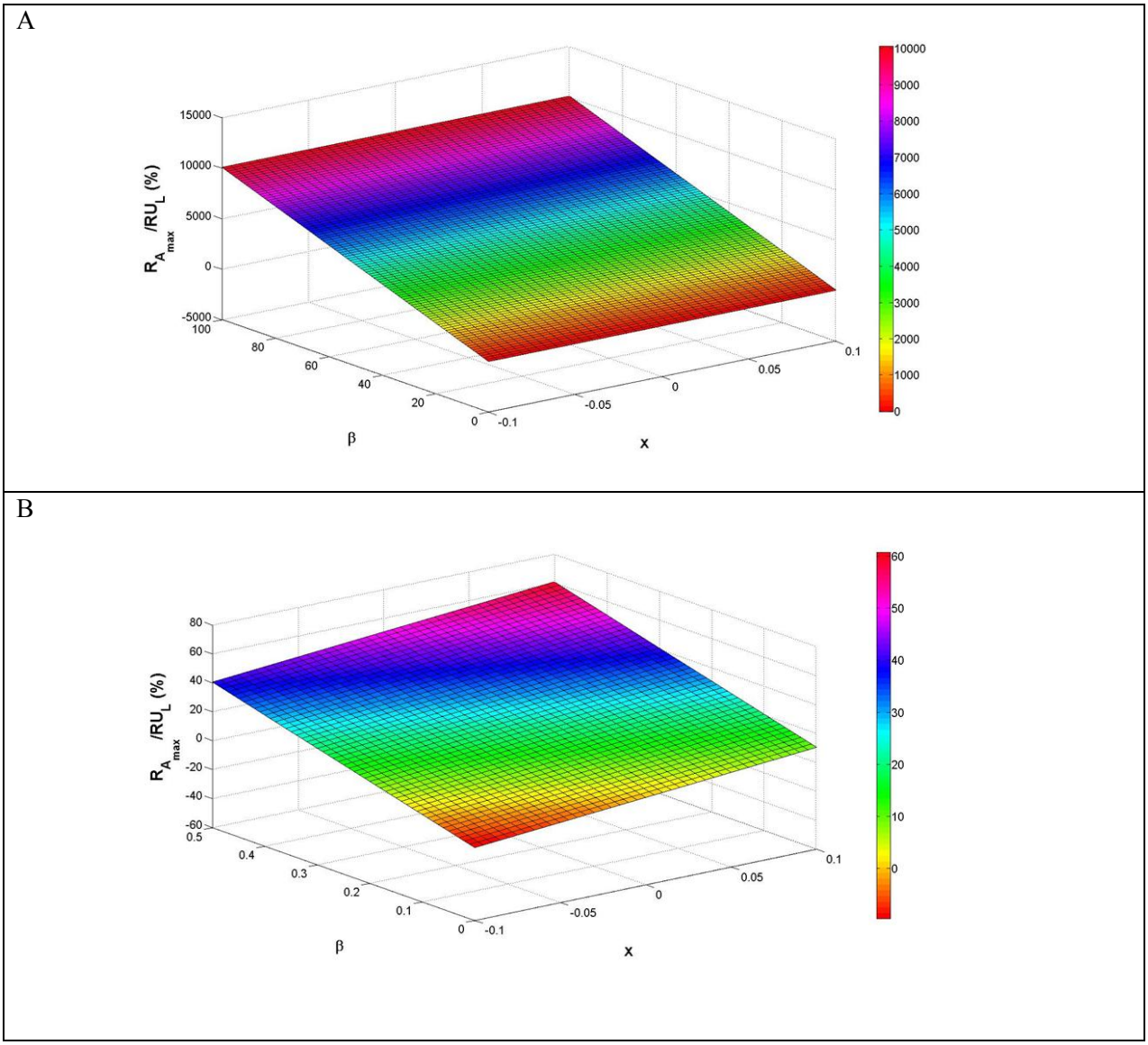

Figure 4. Variation of the R_{Amax}/RU_L ratio in function β and x for A) β ranging from 0 to 100 B) β ranging from 0 to 0.5. d_p=175nm, d_L=5.2 nm, ρ=0.73.

The contribution of the analyte binding on the final receptor structure (R^*_{target}), of the aptamer thickness variation ($R^*_{thickness}$) and of the RII variation (R^*_{RII}) in the experimental maximal SPR signal (eqs 21 to 23) could be evidenced by rearrangement of eq 18 in three adimensionless terms (eq 20) expressed as a function of the same constant R* (eq 24).

$$\frac{R_{A_{\max}}}{RU_L} = R^*_{RII} + R^*_{target} + R^*_{thickness} \quad (20)$$

$$R^*_{target} = \frac{1}{\rho}\frac{1-e^{-\frac{\rho d_L}{d_p}}}{1-e^{-\frac{d_L}{d_p}}}\beta = \beta R^* \quad (21)$$

$$R^*_{thickness} = \frac{1}{\rho}\frac{1-e^{-\frac{\rho d_L}{d_p}}}{1-e^{-\frac{d_L}{d_p}}} - 1 = R^* - 1 \quad (22)$$

$$R^*_{RII} = \frac{1}{\rho}\frac{1-e^{-\frac{\rho d_L}{d_p}}}{1-e^{-\frac{d_L}{d_p}}}x = xR^* \quad (23)$$

$$\text{With } R^* = \frac{1}{\rho}\frac{1-e^{-\frac{\rho d_L}{d_p}}}{1-e^{-\frac{d_L}{d_p}}} \quad (24)$$

While R^*_{target} and R^*_{RII} are proportional to R*, $R^*_{thickness}$ is a translation of R* of -1. R* varies similarly to the R_{Amax}/RU_L ratio in function of d_L and ρ. However, R* variations are small and always positive (from 0.95 % to 1.02 %) in the range of d_L (0 to 10 nm) and ρ (0 to 3) considered here (Figure S6). The contribution of R^*_{target} to the signal is thus always positive. However, the contribution of the R^*_{RII} and $R^*_{thickness}$ could positive or negative, depending on the sign of x and depending of the value of ρ (folding or elongation). Thus, contribution of thickness variation or RII contribution could influence the SPR signal in similar or opposite directions. In the present case (ρ=0.73), R^*_{target}, R^*_{RII} and $R^*_{thickness}$ are valuated to 45%, 42% and 13 % of the final signal respectively. Application of this model allows prediction of the maximal SPR response expected

for different kind of system that undergo conformational transition and thus that do not conformed to a simple recognition as expressed by eq 1. Indeed, conformation transition are widely numerous in biological system and a more general equation taking into account the impact of such modification is of relevant interest.

CONCLUSION

In this paper, we demonstrate the direct SPR detection of a low molecular weight analyte by its receptor presented as a 2-D monolayer. Despite the low density of the receptor, significant SPR signals were obtained and quantification of the interaction was performed. The magnitude of the experimental signal being more than twice the one expected for a simple mass increase of the sensing layer, we further investigated the contribution of conformational transition of the aptamer on SPR signals. We propose a theoretical model to simulate the maximal SPR signal in order to quantify the contribution of target binding and of the conformation changes onto the final response. We highlight that the conformational transition of the aptamer contributes to the SPR signal via two phenomena *i)* a decrease of the sensing layer thickness and *ii)* a deviation of the analyte/receptor complex RII from the sum of the two initial partners RII. In a more general way, this model also allows prediction of the SPR signal for 2D recognition platforms and is applicable to a wide variety of biological recognition system where a conformation transition may occur. We proposed a new equation where the impact of each phenomenon could be evaluated: with or without thickness modification and/or with or without RII deviation. This approach opens new opportunity for using SPR in the physical chemistry domain.

ASSOCIATED CONTENT

Supporting Information. List of abbreviations, SPR experimental data, details for the development of the model for the SPR response (eqs S1 to S15). Supplementary Figures S1 to S6. This material is available free of charge.

AUTHOR INFORMATION

Notes

The authors declare no competing financial interests.

ACKNOWLEDGMENT

This work was partially supported by the French National Research Agency (ANR) under ECSTASE, Contract ANR-10-blan-1517, (Rational design of a sensitive and enantiospecific electrocatalytically-amplified aptasensor for amphetamine derivatives drugs), under "Arcane" LabEx support (ANR-11-LABX-0003-01), and the Joseph Fourier University by AGIR program (Caractérisation et quantification des interactions oligonucléotides-petites molecules). The Nanobio-ICMG platform (FR 2607) is acknowledged for providing synthesis, purification of oligonucleotides and SPR facilities.

REFERENCES

(1) Song, S.; Wang, L.; Li, J.; Zhao, J.; Fan, C. Aptamer-Based Biosensors. *TrAC, Trends Anal. Chem.* **2008,** *27*, 108-117.

(2) Famulok, M.; Mayer, G. Aptamer Modules as Sensors and Detectors. *Acc. Chem. Res.* **2011,** *44*, 1349-1358.

(3) Hong, P.; Li, W.; Li, J. Applications of Aptasensors in Clinical Diagnostics. *Sensors* **2012,** *12*, 1181-1193.

(4) Fang, X.; Tan, W. Aptamers Generated from Cell-SELEX for Molecular Medicine: A Chemical Biology Approach. *Acc. Chem. Res.* **2010,** *43*, 48-57.

(5) Tan, W.; Wang, H.; Chen, Y.; Zhang, X.; Zhu, H.; Yang, C.; Yang, R.; Liu, C. Molecular Aptamers for Drug Delivery. *Trends Biotechnol.* **2011,** *29*, 634-640.

(6) Wu, Z.; Tang, L.-J.; Zhang, X.-B.; Jiang, J.-H.; Tan, W. Aptamer-Modified Nanodrug Delivery Systems. *Acs Nano* **2011,** *5*, 7696-7699.

(7) Palchetti, I.; Mascini, M. Electrochemical Nanomaterial-Based Nucleic Acid Aptasensors. *Anal. Bioanal. Chem.* **2012,** *402*, 3103-3114.

(8) Tombelli, S.; Minunni, M.; Mascini, M. Analytical applications of aptamers. *Biosens. Bioelectron.* **2005,** *20*, 2424-2434.

(9) Iliuk, A. B.; Hu, L.; Tao, W. A. Aptamer in Bioanalytical Applications. *Anal. Chem.* **2011,** *83*, 4440-4452.

(10) Nguyen, V. T.; Kwon, Y. S.; Gu, M. B. Aptamer-Based Environmental Biosensors for Small Molecule Contaminants. *Curr. Opin. Biotechnol.* **2017,** *45*, 15-23.

(11) Gopinath, S. C. B. Biosensing Applications of Surface Plasmon Resonance-Based Biacore Technology. *Sens. Actuators, B* **2010,** *150*, 722-733.

(12) Zhu, Z. L.; Peng, M. X.; Zuo, L. M.; Zhu, Z. T.; Wang, F. W.; Chen, L.; Li, J. H.; Shan, G. Z.; Luo, S. Z. An Aptamer Based Surface Plasmon Resonance Biosensor for the Detection of Ochratoxin A in Wine and Peanut Oil. *Biosens. Bioelectron.* **2015,** *65*, 320-326.

(13) Sun, L. L.; Wu, L. Q.; Zhao, Q. Aptamer Based Surface Plasmon Resonance Sensor for Aflatoxin B1. *Microchim. Acta* **2017,** *184*, 2605-2610.

(14) Wang, J. L.; Munir, A.; Zhou, H. S. Au NPs-Aptamer Conjugates as a Powerful Competitive Reagent for Ultrasensitive Detection of Small Molecules by Surface Plasmon Resonance Spectroscopy. *Talanta* **2009,** *79*, 72-76.

(15) Wang, J. L.; Zhou, H. S. Aptamer-Based Au Nanoparticles-Enhanced Surface Plasmon Resonance Detection of Small Molecules. *Anal. Chem.* **2008,** *80*, 7174-7178.

(16) Durand, G.; Lisi, S.; Ravelet, C.; Dausse, E.; Peyrin, E.; Toulme, J. J. Riboswitches Based on Kissing Complexes for the Detection of Small Ligands. *Angew. Chem. Int. Ed.* **2014,** *53*, 6942-6945.

(17) Durand, G.; Dausse, E.; Goux, E.; Fiore, E.; Peyrin, E.; Ravelet, C.; Toulme, J. J. A Combinatorial Approach to the Repertoire of RNA Kissing Motifs; Towards Multiplex Detection by Switching Hairpin Aptamers. *Nucleic Acids Res.* **2016,** *44*, 4450-4459.

(18) Golub, E.; Pelossof, G.; Freeman, R.; Zhang, H.; Willner, I. Electrochemical, Photoelectrochemical, and Surface Plasmon Resonance Detection of Cocaine Using Supramolecular Aptamer Complexes and Metallic or Semiconductor Nanoparticles. *Anal. Chem.* **2009,** *81*, 9291-9298.

(19) Wang, Q.; Huang, J. H.; Yang, X. H.; Wang, K. M.; He, L. L.; Li, X. P.; Xue, C. Y. Surface Plasmon Resonance Detection of Small Molecule Using Split Aptamer Fragments. *Sens. Actuators, B* **2011,** *156*, 893-898.

(20) Osypova, A.; Thakar, D.; Dejeu, J.; Bonnet, H.; Van der Heyden, A.; Dubacheva, G. V.; Richter, R. P.; Defrancq, E.; Spinelli, N.; Coche-Guérente, L. *et al.* Sensor Based on Aptamer Folding to Detect Low-Molecular Weight Analytes. *Anal. Chem.* **2015,** *87*, 7566-7574.

(21) Balamurugan, S.; Mendez, S.; Balamurugan, S. S.; O'Brien, M. J.; Lopez, G. P. Thermal Response of Poly(N-isopropylacrylamide) Brushes Probed by Surface Plasmon Resonance. *Langmuir* **2003,** *19*, 2545-2549.

(22) Chah, S.; Kumar, C. V.; Hammond, M. R.; Zare, R. N. Denaturation and Renaturation of Self-Assembled Yeast iso-1-Cytochrome C on Au. *Anal. Chem.* **2004,** *76*, 2112-2117.

(23) Sarkar, D.; Somasundaran, P. Conformational Dynamics of Poly(acrylic acid). A Study Using Surface Plasmon Resonance Spectroscopy. *Langmuir* **2004,** *20*, 4657-4664.

(24) Chen, L.-Y. Monitoring Conformational Changes of Immobilized RNase A and Lysozyme in Reductive Unfolding by Surface Plasmon Resonance. *Anal. Chim. Acta* **2009,** *631*, 96-101.

(25) Nilebäck, E.; Westberg, F.; Deinum, J.; Svedhem, S. Viscoelastic Sensing of Conformational Changes in Plasminogen Induced upon Binding of Low Molecular Weight Compounds. *Anal. Chem.* **2010,** *82*, 8374-8376.

(26) Gestwicki, J. E.; Hsieh, H. V.; Pitner, J. B. Using Receptor Conformational Change to Detect Low Molecular Weight Analytes by Surface Plasmon Resonance. *Anal. Chem.* **2001,** *73*, 5732-5737.

(27) Dell'Orco, D.; Muller, M.; Koch, K. W. Quantitative Detection of Conformational Transitions in a Calcium Sensor Protein by Surface Plasmon Resonance. *Chem. Commun.* **2010,** *46*, 7316-7318.

(28) Dell'Orco, D.; Sulmann, S.; Linse, S.; Koch, K. W. Dynamics of Conformational Ca^{2+}-Switches in Signaling Networks Detected by a Planar Plasmonic Device. *Anal. Chem.* **2012,** *84*, 2982-2989.

(29) Sulmann, S.; Dell'Orco, D.; Marino, V.; Behnen, P.; Koch, K. W. Conformational Changes in Calcium-Sensor Proteins under Molecular Crowding Conditions. *Chem. Eur. J.* **2014,** *20*, 6756-6762.

(30) Dell'Orco, D.; Koch, K. W. Fingerprints of Calcium-Binding Protein Conformational Dynamics Monitored by Surface Plasmon Resonance. *ACS Chem. Biol.* **2016,** *11*, 2390-2397.

(31) Sandrin, L.; Thakar, D.; Goyer, C.; Labbe, P.; Boturyn, D.; Coche-Guerente, L. Controlled Surface Density of RGD Ligands for Cell Adhesion: Evidence for Ligand Specificity by Using QCM-D. *J. Mater. Chem. B* **2015,** *3*, 5577-5587.

(32) Rich, R. L.; Myszka, D. G. Advances in Surface Plasmon Resonance Biosensor Analysis. *Curr. Opin. Biotechnol.* **2000,** *11*, 54-61.

(33) Challier, L.; Miranda-Castro, R.; Barbe, B.; Fave, C.; Limoges, B.; Peyrin, E.; Ravelet, C.; Fiore, E.; Labbé, P.; Coche-Guérente, L. *et al.* Multianalytical Study of the Binding between a Small Chiral Molecule and a DNA Aptamer: Evidence for Asymmetric Steric Effect upon 3′- versus 5′-End Sequence Modification. *Anal. Chem.* **2016,** *88*, 11963-11971.

(34) Lin, P.-H.; Yen, S.-L.; Lin, M.-S.; Chang, Y.; Louis, S. R.; Higuchi, A.; Chen, W.-Y. Microcalorimetrics Studies of the Thermodynamics and Binding Mechanism Between L-Tyrosinamide and Aptamer. *J. Phys. Chem. B* **2008,** *112*, 6665-6673.

(35) Ruta, J.; Perrier, S.; Ravelet, C.; Fize, J.; Peyrin, E. Noncompetitive Fluorescence Polarization Aptamer-based Assay for Small Molecule Detection. *Anal. Chem.* **2009,** *81*, 7468-7473.

(36) Challier, L.; Mavre, F.; Moreau, J.; Fave, C.; Schoellhorn, B.; Marchal, D.; Peyrin, E.; Noel, V.; Limoges, B. Simple and Highly Enantioselective Electrochemical Aptamer-Based Binding Assay for Trace Detection of Chiral Compounds. *Anal. Chem.* **2012,** *84*, 5415-5420.

(37) Nguyen, B.; Tanious, F. A.; Wilson, W. D. Biosensor-Surface Plasmon Resonance: Quantitative Analysis of Small Molecule-Nucleic Acid Interactions. *Methods* **2007,** *42*, 150-161.

(38) Liang, D. H.; Luu, Y. K.; Kim, K. S.; Hsiao, B. S.; Hadjiargyrou, M.; Chu, B. In Vitro Non-Viral Gene Delivery With Nanofibrous Scaffolds. *Nucleic Acids Res.* **2005,** *33*.

(39) Lai, E.; van Zanten, J. H. Monitoring DNA/poly-L-Lysine Polyplex Formation with Time-Resolved Multiangle Laser Light Scattering. *Biophys. J.* **2001,** *80*, 864-873.

(40) Davis, T. M.; Wilson, W. D. Determination of the Refractive Index Increments of Small Molecules for Correction of Surface Plasmon Resonance Data. *Anal. Biochem.* **2000,** *284*, 348-353.

(41) Tumolo, T.; Angnes, L.; Baptista, M. S. Determination of the Refractive Index Increment (dn/dc) of Molecule and Macromolecule Solutions by Surface Plasmon Resonance. *Anal. Biochem.* **2004,** *333*, 273-279.

(42) Jung, L. S.; Campbell, C. T.; Chinowsky, T. M.; Mar, M. N.; Yee, S. S. Quantitative Interpretation of the Response of Surface Plasmon Resonance Sensors to Adsorbed Films. *Langmuir* **1998,** *14*, 5636-5648.

(43) Schoch, R. L.; Kapinos, L. E.; Lim, R. Y. H. Nuclear Transport Receptor Binding Avidity Triggers a Self-Healing Collapse Transition in FG-Nucleoporin Molecular Brushes. *Proc. Natl. Acad. Sci. U. S. A.* **2012,** *109*, 16911-16916.

(44) Defeijter, J. A.; Benjamins, J.; Veer, F. A. Ellipsometry as a Tool to Study Adsorption Behaviorof Synthetic and Biopolymers at Air-Water Interface. *Biopolymers* **1978,** *17*, 1759-1772.

(45) Bornhop, D. J.; Kammer, M. N.; Kussrow, A.; Flowers, R. A.; Meiler, J. Origin and Prediction of Free-Solution Interaction Studies Performed Label-Free. *Proc. Natl. Acad. Sci. U. S. A.* **2016,** *113*, E1595-E1604.

TOC GRAPHICS